

Liquid–Vapor Interface of Methanol–Water Mixtures: A Molecular Dynamics Study

Tsun-Mei Chang*

Department of Chemistry, University of Wisconsin, Parkside, 900 Wood Road, Box 2000,
Kenosha, Wisconsin 53141-2000

Liem X. Dang

Chemical Sciences Division, Pacific Northwest National Laboratory, Richland, Washington 99352

Received: September 24, 2004; In Final Form: November 11, 2004

Molecular dynamics simulations were carried out to investigate the structural and thermodynamic properties and variations in the dipole moments of the liquid–vapor interfaces of methanol–water mixtures. Various methanol–water compositions were simulated at room temperature. We found that methanol tends to concentrate at the interface, and the computed surface tension shows a composition dependence that is consistent with experimental measurements. The methanol molecule shows preferred orientation near the interface with the methyl group pointing into the vapor phase. The methanol in the mixture is found to have larger dipole moments than that of pure liquid methanol. The strong local field induced by the surrounding water molecules is partly the reason for this difference. The dependence of hydrogen-bonding patterns between methanol and water on the interface and the composition of the mixture is also discussed in the paper.

I. Introduction

Understanding the interfacial properties of liquid–vapor interfaces is of great interest because these properties play key roles in many areas of science including chemistry, physics, material sciences, and biology. For example, developing an understanding of the liquid–vapor interface of aqueous solutions is crucial in solving environmental problems such as acid rain or water pollution.¹ Understanding how chemical species adsorb and behave at the liquid–vapor interfaces has important implications in wetting, coating, and form formation.²

Because of the intrinsic asymmetry of the liquid–vapor interface, it is expected that the chemical and physical properties of interfaces will be different than those of bulk systems. Recent advances in the modern experimental techniques have made it possible to examine the structural and dynamical properties at liquid interfaces. These techniques include nonlinear-optical spectroscopy (second harmonic generations or sum frequency generations),^{3,4} X-ray diffraction and reflection,⁵ and neutron reflection.⁶ However, interpretation of these experimental data is subject to the underlying physical models, and the ability to directly probe the interfacial properties is limited. Theoretical approaches, especially computer simulations, have proven to be useful tools in providing detailed information on a molecular level of the structural, thermodynamic, and dynamical properties at liquid interfaces.^{7,8}

In this study, we focused our attention on the methanol–water interface. Methanol, being the simplest alcohol, has been a subject of many theoretical and experimental studies.^{9–14} Each methanol molecule contains two distinct parts: the methyl group, which is hydrophobic, and the hydroxide group, which is hydrophilic and is able to form hydrogen bonds. Therefore, when methanol is mixed with water, the resulting solution would be expected to deviate from the expected, ideal behavior and

may show unusual properties. Recently, there have been many experimental and theoretical studies devoted to the study of molecular structures of methanol–water solutions.^{15–26} Matsumoto et al. performed molecular dynamics (MD) simulations for the liquid–vapor interfaces of methanol–water mixtures at various compositions.¹⁷ They found that the interface is saturated with methanol molecules, a result that agrees with those obtained from experimental work. Simulation studies by Ferrario and co-workers,²⁷ as well as by Laaksonen and co-workers,¹⁹ provided information on the structures and dynamics of hydrogen-bonding patterns in methanol–water mixtures at a molecular level. Neutron-scattering experiments by Soper and co-workers were carried out to investigate the molecular structural properties of concentrated alcohol/water solutions, and a tendency for methanol to segregate in aqueous solutions was observed.^{20–22,37} By use of X-ray emission spectroscopy, Guo and co-workers also found that water and methanol do not mix completely at the microscopic level.²³ These studies have contributed significantly to our understanding of methanol–water mixtures.

As part of ongoing research of liquid interfaces, we studied the equilibrium properties of the liquid–vapor interfaces of methanol–water mixtures using MD techniques. The dynamical properties of this system are deferred for future work. This paper is organized as follows. The computational details of our MD simulations are briefly described in section II. Our simulation results are presented and discussed in section III, and our conclusions are given in section IV.

II. Computational Methods

In our study, we used previously developed many-body polarizable potential models to describe methanol–water intermolecular interactions.^{28,29} MD simulations were performed on pure methanol, pure water, and seven methanol–water mixtures with the methanol mole fraction, x_M , ranging from 0.05 to 0.95 M. The number of water and methanol molecules used

* Author to whom correspondence may be addressed. E-mail: chang@uwp.edu.

TABLE 1: Simulation Details^a

x_M	0.05	0.10	0.25	0.50	0.75	0.90	0.95	1.00
N_{water}	950	810	600	350	150	45	26	0
N_{methanol}	50	90	200	350	450	495	494	500

^a x_M is the mole fraction of methanol in the liquid phase. N_{water} and N_{methanol} are the numbers of water and methanol molecules used in the simulations.

in the simulations is listed in Table 1. The systems were prepared by starting with a liquid slab of equilibrated methanol–water mixture in a simulation cell of linear dimensions roughly equal to $32 \times 32 \times 96 \text{ \AA}^3$. This cell created two mixture–vapor interfaces that were perpendicular to the z -axis. During the entire simulation, a periodic boundary condition was applied in all three spatial directions. The simulations were carried out in a constant volume–temperature (NVT) ensemble. The temperature of the system was maintained at 298 K by coupling the water and CH_3OH to separate external thermal baths with a time constant of 0.2 ps via the Berendsen scheme.³⁰ The initial velocities for each atom were taken from a Maxwell–Boltzmann distribution corresponding to the desired simulation temperature. All bond lengths in the system were constrained by the SHAKE algorithm.³¹ A time step of 2 fs was used to integrate the equations of motion. To be consistent with the procedure in the potential development, all simulations used a molecular cutoff distance of 9 Å for the nonbonded interactions. The system was equilibrated for 300 ps prior to a 1-ns simulation period during which data was collected.

III. Results and Discussion

A. Density Profile. In Figure 1 the calculated mass densities of methanol (ρ_M), water (ρ_W), and the mixture (ρ_{tot}) are shown as a function of the z coordinate normal to the interface for various compositions. These densities are evaluated using liquid slabs of 1-Å thickness parallel to the interface and clearly show the existence of two distinct liquid–vapor interfaces at all compositions. Between the two interfaces, there is a stable region with bulklike density. The mixture density profile can be fit into a hyperbolic tangent functional form³²

$$\rho(z) = \frac{1}{2}(\rho_L + \rho_V) - \frac{1}{2}(\rho_L - \rho_V) \tanh[(z - z_0)/d] \quad (1)$$

where ρ_L and ρ_V are the liquid and vapor densities, respectively, z_0 is the position of the Gibbs’s dividing surface, and d estimates the thickness of the interface. The best-fit curves for the solution density profiles are also shown in Figure 1. The estimates of the liquid densities, the locations of the Gibbs’s dividing surfaces, and interfacial widths obtained from the fits are summarized in Table 2. Because methanol molecules have weaker molecular interactions and are more volatile, it is found that the liquid–vapor interfacial width of pure methanol is wider than that of water. Therefore, the interface width increases with increasing methanol concentration.

In general, the mixture density profiles are quite smooth, and no long-range structures are expected near the interface. However, the individual densities for methanol and water are less uniform across the surface normal direction. In particular, we found when there is an enrichment of water density, the methanol density is reduced and vice versa. This finding suggests there may be a local clustering of methanol and water molecules and is consistent with the recent experimental results that molecular segregation occurs even for the shortest alcohol in aqueous solution.^{21,23} Additionally, the density ratios of methanol to the mixture as a function of its z position is found

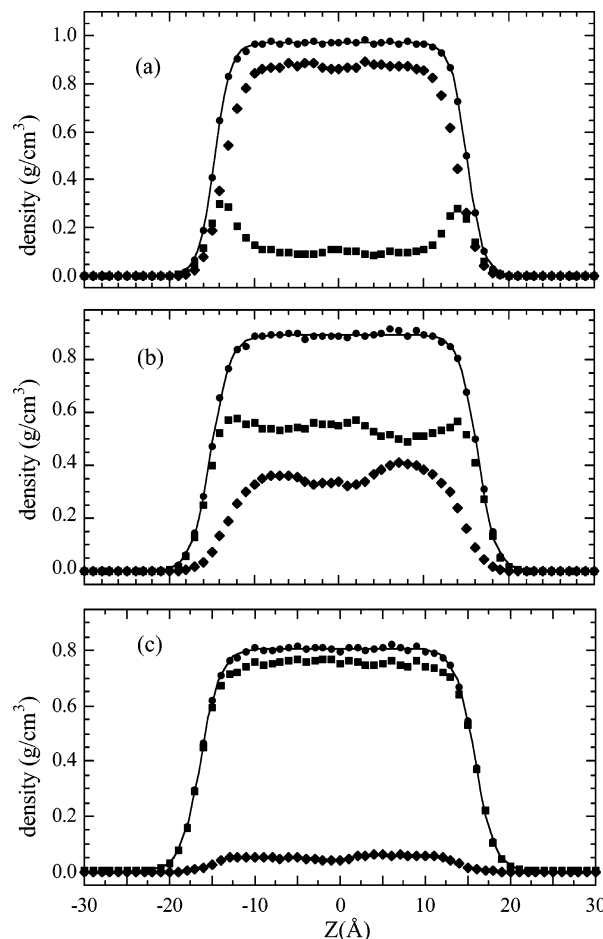


Figure 1. The computed density profiles of methanol (squares), water (diamonds), and the mixture (circles) at room temperature. The mole fraction of methanol in the bulk, x_M , is (a) 0.1, (b) 0.5, and (c) 0.9. The solid line indicates the best fit to the mixture density profile.

TABLE 2: Fitted Bulk Mixture Density, Interfacial Width, and Location of the Gibbs’s Dividing Surfaces from the z -Dependent Density Profiles at Various Methanol Concentrations

x_M	$\rho_{\text{tot}} (\text{g/cm}^3)$	$Z_{\text{Gibbs}} (\text{\AA})$	$d (\text{\AA})$
0.05	0.979	± 15.8	1.85
0.10	0.971	± 14.9	1.89
0.25	0.942	± 15.5	1.94
0.50	0.896	± 15.7	2.20
0.75	0.840	± 16.0	2.26
0.90	0.804	± 16.3	2.73
0.95	0.797	± 14.5	2.70

to increase significantly near the interface at all compositions, suggesting a strong tendency of methanol molecules to concentrate at the interface. Alcohol molecules are known to be surface active in aqueous solutions. By pointing the hydrophobic tail into the vapor phase, they gain better molecular interaction and thus reduce surface free energy. To verify this finding, we examined the atomic number profile for C and O atoms of methanol as a function of the z coordinate. The probability of finding C atoms is higher than that of finding O atoms in the interface region, supporting the idea that the methyl group is preferentially pointing toward the vapor phase.

B. Surface Tension. We evaluated the surface tension, γ , of the methanol–water mixtures as a function of methanol mole fraction, x_M . The surface tension, which is the surface free energy associated with creating new surface area, can be

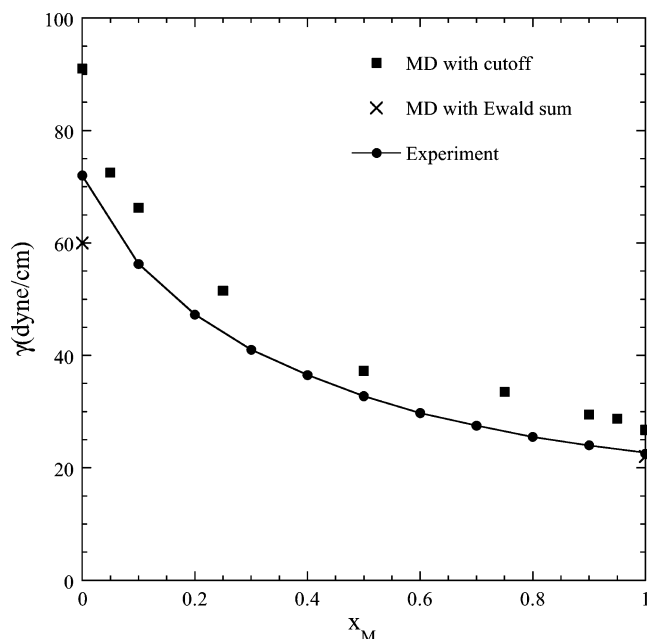


Figure 2. Surface tension of methanol–water mixtures as a function of the methanol mole fraction.

computed as the difference between the pressure components in the directions parallel to and perpendicular to the interface³³

$$\gamma = \frac{1}{2} \left(\frac{p_{xx} + p_{yy}}{2} - p_{zz} \right) L_z \quad (2)$$

In eq 2, $p_{\alpha\alpha}$ ($\alpha = x, y, \text{ or } z$) is the $\alpha\alpha$ element of the pressure tensor, and L_z is the linear dimension of the simulation cell in the z direction. According to the virial equation, the $\alpha\beta$ element of the pressure tensor is

$$p_{\alpha\beta} = \frac{1}{V} \left(\sum_{i=1}^N m_i v_{i\alpha} v_{i\beta} + \frac{1}{2} \sum_{i'=1}^{N'} \sum_{j'=1}^{N'} F_{i'j'\alpha} r_{ij\beta} \right) \quad (3)$$

where N and N' are the numbers of molecules and atoms, respectively. V is the total volume of the system, m_i is the mass of molecule i , and $v_{i\alpha}$ is the α component of the center-of-mass velocity of molecule i , $F_{i'j'\alpha}$ is the α component of the force exerted on atom i' of molecule i due to atom j' of molecule j , and $r_{ij\beta}$ is the β component of the vector connecting the center of mass of molecules i and j . The calculated surface tension is shown in Figure 2 along with the experimental results. The calculated values of the surface tension are about 10–30% higher than the experimental values, which is expected because the potential models we used predict a higher surface tension for the liquid–vapor interfaces of pure methanol and pure water. In general, the overall dependence of the surface tension on the mixture composition agrees well with the experimental trend. When a small amount of methanol is added to the water, the surface tension significantly decreases, a finding that we attribute to the strong tendency for methanol to concentrate at the interface. We have also included in Figure 2 two additional surface tension calculations of liquid water and liquid methanol using Ewald summation techniques. As expected, the computed surface tensions were sensitive to the treatment of long-range forces.

C. Interfacial Structures. We began our study of interfacial structures by investigating the orientation of methanol and water molecules at the interface. This orientation plays an important role in the reactivity of the interface. Additionally, we studied

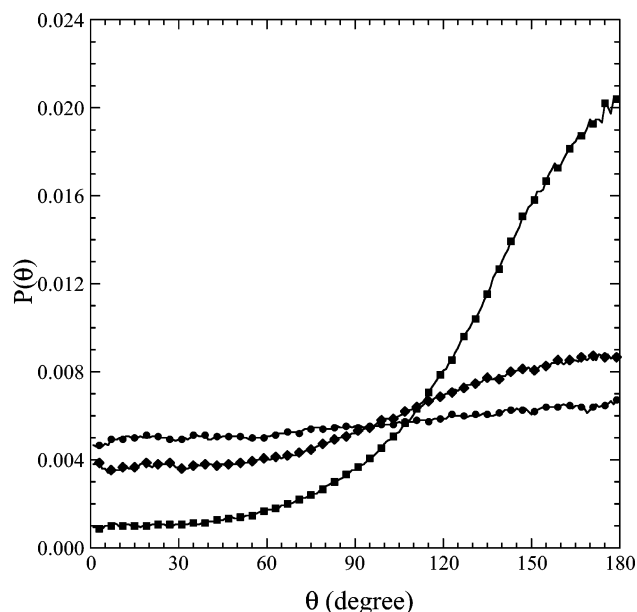


Figure 3. Orientational distribution of methanol as a function of its position relative to the interface. The angle, θ , is between the surface normal direction and the intramolecular O–C bond of the methanol molecule. The data points correspond to the methanol molecules located at the Gibbs's dividing surface (squares), 4 Å (diamonds), and 8 Å (circles) away from the dividing surface into the liquid region for a solution with $x_M = 0.5$.

how the local structure of water and methanol changed from the bulk region to the interface by examining radial distribution functions (RDF).

1. Methanol Orientation and Local Structures. Figure 3 shows the probability distributions for the angle between the surface normal and the bond axis pointing from the O atom to the C atom of methanol as a function of the methanol z coordinate for the upper interface of a $x_M = 0.5$ solution. Similar behavior has been observed for all other concentrations. In all cases, the orientational distribution functions show a uniform distribution (indicated by a straight line) for methanol molecules in the liquid region. As the methanol molecule moves from the bulk region into the interfacial region, the angular probability deviates from the uniform distribution and shows a strong peak near 180° . It is evident that there is a preferred orientational order and a tendency for the CO bond of surface methanol molecules to lie parallel with the surface normal direction, with the C atom pointing into the vapor phase. This finding agrees with the sum-frequency generation experimental results that showed a methyl group of methanol projecting out to the vapor phase.^{16,34} We also observed that the peak becomes broader for more concentrated solutions, suggesting that the surface structure becomes less ordered with increasing methanol concentration, as suggested by other recent studies.^{16,34}

The change in the local structures of methanol molecules from the bulk region to the interface can be examined in terms of the atomic RDFs as a function of the methanol z coordinate. In Figure 4, the calculated O–O RDFs of methanol are shown for solutions with methanol mole fractions, $x_M = 0.1$. These RDFs give the probability of finding the O atom of methanol molecules at a distance r away from an O atom of one methanol molecule. For methanol in the bulk region, the RDF will approach the methanol mole fraction of the mixture at large separations. The intensity of these radial distribution functions will be reduced for a methanol molecule located near the interface due to the decreasing number density of CH_3OH in the interfacial regions. In Figure 4, the main features of the RDFs are similar from the

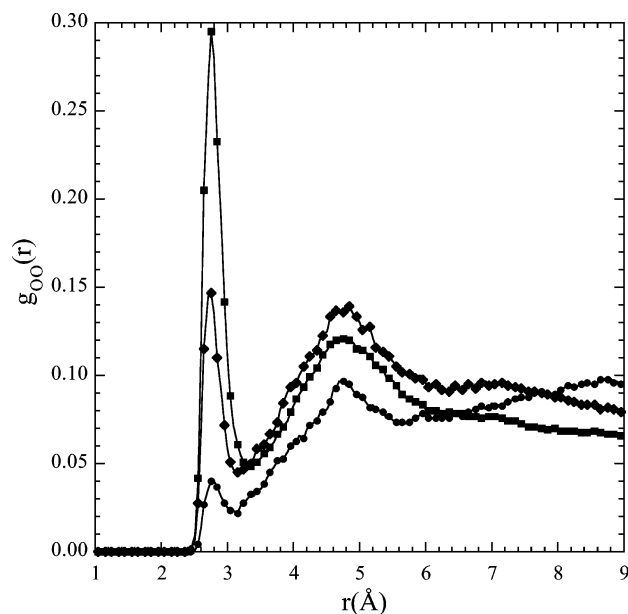


Figure 4. The O–O radial distribution function for methanol as a function of its location relative to the interface for a solution of $x_M = 0.1$. The three curves correspond to the methanol molecules located at the Gibbs's dividing surface (squares), 4 Å (diamonds), and 8 Å (circles) away from the dividing surface into the liquid region.

bulk region to the interface, suggesting that the local atomic arrangement of CH_3OH remains unaffected by the presence of the interface. However, the height of the first peak in the O–O RDF increases significantly as methanol approaches the interface. This result is consistent with the idea that there is a local clustering of methanol at the interface and that the order of the surface structure is enhanced. This trend becomes less pronounced for more concentrated solutions. While the position of the first peak in the O–O RDF remains unchanged as the methanol concentration increases, the location of the second peak gradually shifts to larger separations, possibly caused by the presence of the intervening water molecules. This result suggests that a tighter second solvation shell of methanol exists in the dilute solutions, which may come from the local clustering of methanol molecules in the mixtures.

2. Water Orientation and Local Structures. Because of the directional interactions between water molecules, they are observed to show preferred orientational order at the liquid-vapor interface. Figure 5 shows the probability distributions for the angle between the water C_{2v} molecular axis (permanent dipole direction) and the z -axis as a function of the z coordinate for a 0.1 M methanol solution. In the bulk region, the angular distributions are quite uniform. As water approaches the interface, the angular distribution deviates from the uniform distribution, and the probability of the angle between the water molecular axis and the interface normal around 90° increases greatly, which suggests that the water permanent dipoles prefer to lie parallel to the interface. Similar behavior has also been observed in other water interfaces^{7,35} and is attributed to the idea that the interface of water has icelike structure.³⁶

We computed water O–O radial distribution functions as a function of its z coordinate. At each composition, little change is observed for the peak positions of the water RDFs regardless of water location, suggesting that the local structure of water is unaffected by the presence of the interface. However, it is noted that, as the methanol concentration increases, the location of the second peak of the water O–O RDF shifts to larger distances. This result clearly indicates that the presence of

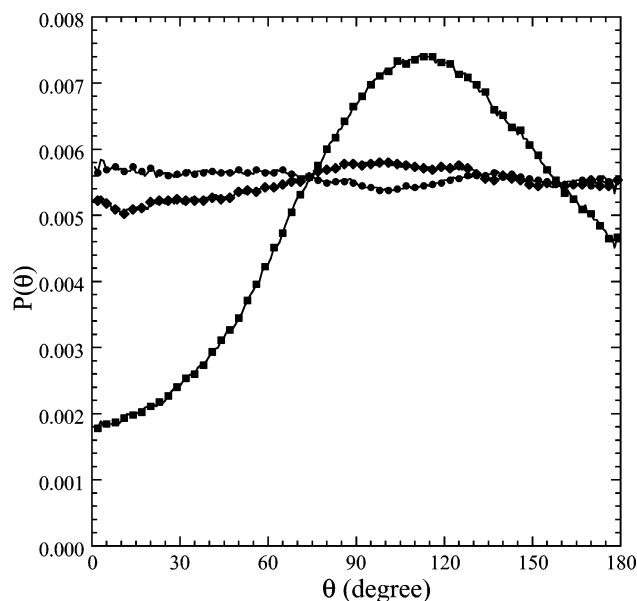


Figure 5. Orientational distribution of water as a function of its position relative to the interface. The angle, θ , is between the surface normal direction and the intramolecular C_{2v} molecular axis of water molecule. The data points correspond to the water molecules located at the Gibbs's dividing surface (squares), 4 Å (diamonds), and 8 Å (circles) away from the dividing surface into the liquid region for a 0.1 M solution.

methanol molecules has changed the local molecular configurations between water molecules.

D. Hydrogen Bonding. 1. Water–Water Hydrogen Bonding. Both methanol and water are capable of forming hydrogen bonds. By examination of the hydrogen-bonding patterns in the mixture, insight can be gained into the effects of interface and mixing on the molecular interaction. In this study, a geometric criterion is used to define the hydrogen bond. Two molecules are considered hydrogen bonded when the intermolecular O–H distance is less than the distance of the first minimum of the O–H radial distribution function. In Figure 6a, we show a plot of the average number of hydrogen bonds per molecule between water molecules as a function of the molecular location normal to the interface at $x_M = 0.05, 0.10, 0.25$, and 0.50 . In the bulk liquid region, the number of hydrogen bonds per water molecule is roughly constant and decreases with increasing methanol concentrations. This is clearly caused by the decrease in the availability of water molecules for hydrogen bonding. As water molecules approach the interface, the number of hydrogen bonds decreases monotonically, which results from the reduced density in the interfacial region.

In addition to the absolute number of hydrogen bonds, we also were interested in determining to what degree the hydrogen bonding was affected by the presence of the interface and by mixing. We evaluated this quantity by dividing the average number of hydrogen bonds by the average number of water molecules in the first solvation shell (defined by the first minimum in the O–O radial distribution function). The percentage of the hydrogen bonding per water molecule is depicted in Figure 6b as a function of its z coordinate. We found that the degree of hydrogen bonding increases near the interface. This behavior indicates that the interface enhances hydrogen bonding, and these results are similar to those obtained from previous MD simulations of the water–dimethyl sulfoxide (DMSO) liquid–vapor interface⁷ and the water–carbon tetrachloride liquid–liquid interface.³⁵ When methanol is added to water, although the number of hydrogen bonds per water molecule decreases (from ~ 3.8 for $x_M = 0.05$ to ~ 2.3 for $x_M = 0.5$), the

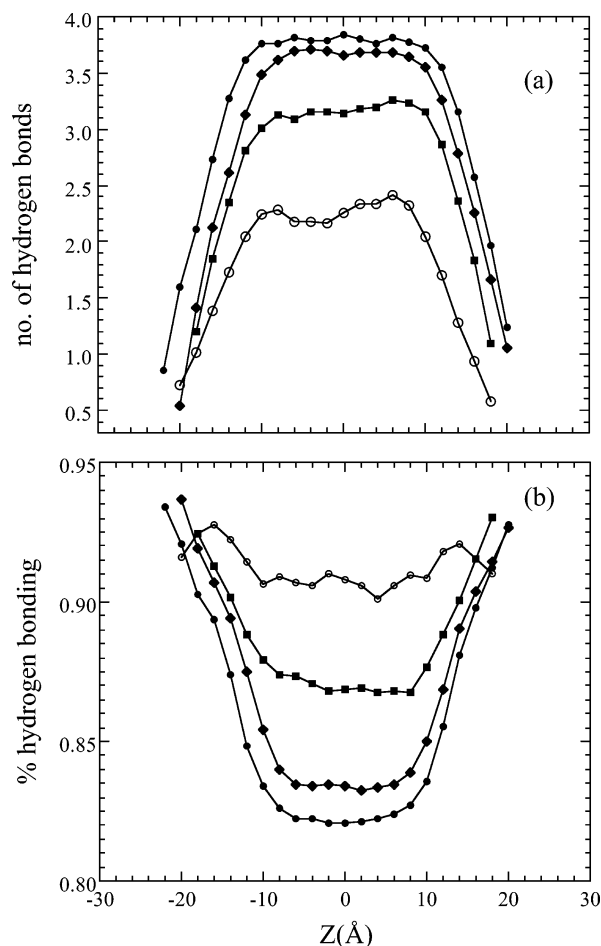


Figure 6. Hydrogen-bonding analysis between water molecules. (a) Number of hydrogen bonds per methanol molecule as a function of the location along the interface normal. The four curves correspond to methanol–water mixtures with $x_M = 0.05$ (solid circles), 0.10 (diamonds), 0.25 (squares), and 0.50 (open circles), respectively. (b) The degree of hydrogen bonding of water as a function of its z coordinate, which is defined as the number of hydrogen bonds divided by the number of water molecules in the first solvation shell.

degree of hydrogen bonding actually increases as the methanol mole fraction increases. This result clearly indicates that the addition of methanol molecules enhances the water–water hydrogen bond. Interestingly, the effect of the interface on the degree of hydrogen bonding decreases by the addition of methanol molecules. It is evident from Figure 6 that, for the mixture with $x_M = 0.05$, the percent hydrogen bonding increases from about 0.8 in the bulk region to 0.95 at the interface, while the degree of hydrogen bonding stays about 0.9 when the mole fraction of methanol increases to 0.5. Benjamin has observed similar behavior in his MD study of the DMSO–water system.⁷ He found that the interface generally enhances the percent hydrogen bonding of water to about 90%. Because the addition of methanol to water already increases the degree of hydrogen bonding in the bulk phase, the enhancement due to the interface becomes less obvious.

2. Methanol–Methanol Hydrogen Bonding. In Figure 7, the hydrogen-bonding pattern between methanol molecules is examined. In our study, we found the number of hydrogen bonds per methanol molecule first increases as the methanol molecule approaches the liquid–vapor interface from the bulk region and then decreases monotonically as it passes the Gibbs dividing

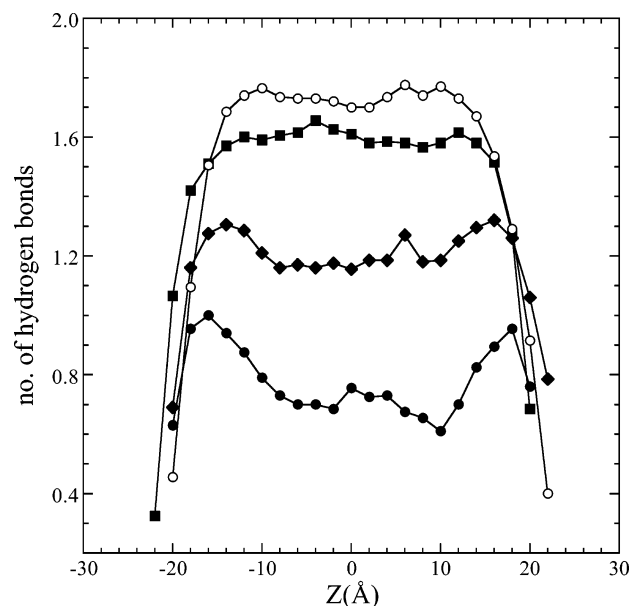


Figure 7. Hydrogen-bonding analysis between methanol molecules. Number of hydrogen bonds per methanol molecule as a function of the location along the interface normal. The four curves correspond to methanol–water mixtures with $x_M = 0.50$ (solid circles), 0.75 (diamonds), 0.90 (squares), and 0.95 (open circles), respectively.

surface. This behavior can be explained by the increase in the number density near the interface from the surface enrichment of methanol and the decrease in number density into the vapor phase. The degree of hydrogen bonding per methanol molecule is also evaluated as a function of its z coordinate. Here, the interface is again observed to enhance the hydrogen bonding between methanol molecules. Interestingly, when the degree of hydrogen bonding of methanol is examined as a function of its concentration, we found that the behavior of the methanol molecule is opposite to that of water. The introduction of water in liquid methanol reduces the methanol–methanol hydrogen bonding. This makes sense because the methanol–water interaction is stronger than methanol–methanol interaction. Thus, the hydroxide group in methanol will preferentially interact with water to reduce the energy of the system.

3. Methanol–Water Hydrogen Bonding. We also investigated the hydrogen bonding between methanol and water. The results of the number of hydrogen bonds per methanol molecule are shown in Figure 8. This quantity is roughly constant in the bulk region and decreases monotonically into the interface region due to the reduced number density. The number of hydrogen bonds between methanol and water decreases from ~ 2.1 for $x_M = 0.25$ solution to ~ 0.9 for $x_M = 0.75$ solution. In general, the composition dependence on the hydrogen bonding in the mixtures behaves similarly to that in the bulk mixtures.²⁷ We found the z dependence of the degree of methanol–water hydrogen bonding behaves in a manner that is similar to that of the water–water hydrogen bonds. The probability of hydrogen bonding between methanol and water molecules is enhanced at the interface and by mixing methanol with water.

E. Variation of Dipole Moments. To examine the influence of the interface and mixing on the electrostatic properties of methanol–water mixtures, we calculated the total dipole moments of water and methanol molecules as a function of the z -axis parallel to the interface for several compositions. The average dipole moments of water molecules in the bulk have an average value of 2.7 D and decrease monotonically as they

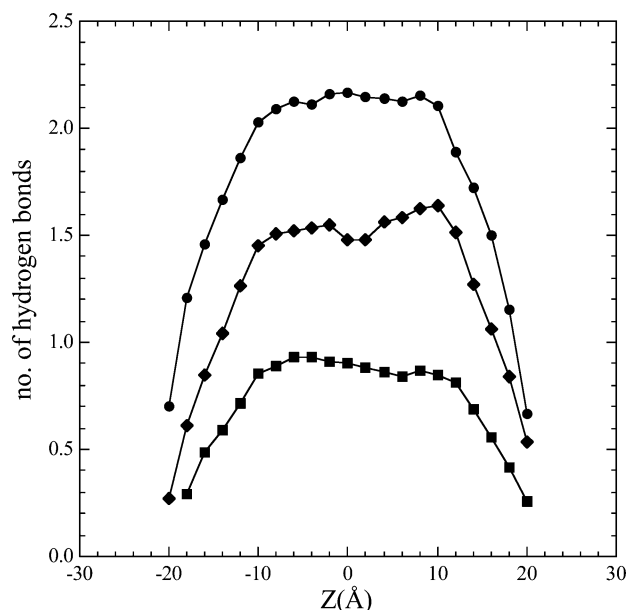


Figure 8. Hydrogen-bonding analysis between methanol and water molecules. Number of hydrogen bonds per methanol molecule between methanol and water as a function of the location along the interface normal. The three curves correspond to methanol–water mixtures with $x_M = 0.25$ (solid circles), 0.50 (diamonds), and 0.75 (squares), respectively.

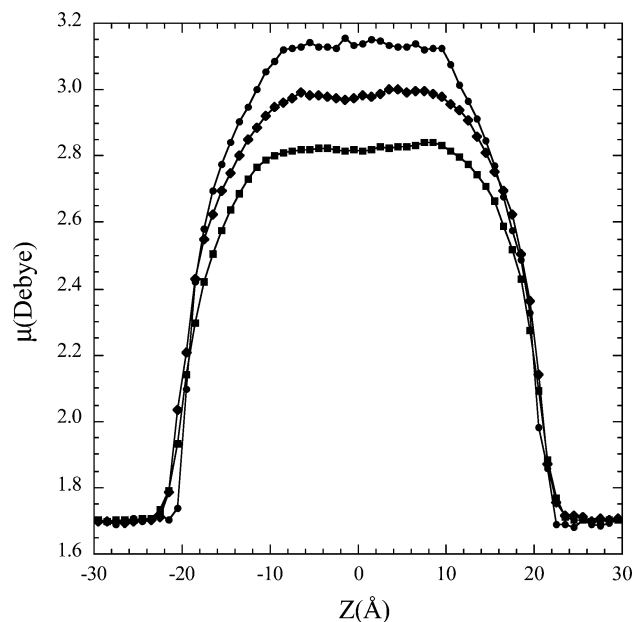


Figure 9. The total dipole moment of methanol molecule as a function of the z axis. The data points corresponds to the methanol mole fraction, $x_M = 0.1$ (circles), 0.5 (diamonds), and 0.9 (squares), respectively.

approach the interface and reach a value close to their gas-phase dipole moments. These results are expected, and a similar trend has been observed for the water–carbon tetrachloride liquid–liquid interface.³⁵ They are caused, in part, by the redistribution of the electric field around these water molecules. For methanol, the average dipole moment is within the 2.8–3.2 D range in the bulk region as shown in Figure 9. These values, which are larger than those of pure bulk methanol, increase as water concentration increases, which may come from the strong local electric field induced by water molecules. Near the interface, the average dipole moments of methanol molecules reduce to the gas-phase value.

IV. Conclusions

By use of classical MD simulation techniques, we explored the structures, thermodynamics, and electrostatic properties of liquid–vapor interfaces in methanol–water mixtures of varying compositions.

The computed density profile shows an enrichment of methanol density near the interface, which is in good agreement with results obtained experimentally. From a detailed analysis, the interfacial thickness is observed to increase with increasing methanol concentration. The computed composition-dependence of the surface tension is consistent with the experimental trend; the surface tension of the solution is greatly reduced by adding a small amount of methanol to water.

The results of the RDFs and the angular probability distributions provide information on the structures of methanol–water mixtures. The results of orientational distribution functions indicate that methanol and water near the interface both show a preferred orientational order that is induced by the presence of the liquid–vapor interface. On the other hand, the interface does not seem to affect the local molecular configurations of the water or methanol molecules. By a mix of water with methanol, we found that the solvation structures were modified as indicated by the shift of the peak position of the atomic radial distribution functions.

The interface and the degree of mixing also affected the hydrogen bonding in methanol–water mixtures. Although the number of hydrogen bonds per molecule decreases near the interface because of the reduced number densities, the interface actually reinforces the degree of hydrogen bonding to reduce surface energy. By variation of the methanol composition, we observed that water–water, methanol–methanol, and water–methanol hydrogen bonding was enhanced as the methanol concentration increased.

The computed average dipole moments of methanol and water molecules near the interface were found to be close to their gas-phase values. While water molecules located far from the interface have dipole moments corresponding to values found in the bulk region, the dipole moments of methanol molecules become larger than the bulk region value because of mixing with water molecules. This behavior can be attributed to the stronger local electric field induced by the surrounding water molecules.

Acknowledgment. Part of this work was performed at Pacific Northwest National Laboratory (PNNL) under the auspices of the Division of Chemical Sciences, Office of Basic Energy Sciences, U.S. Department of Energy. Battelle operates PNNL for the Department of Energy. Computer resources were provided by the Division of Chemical Sciences and by the Scientific Computing Staff, Office of Energy Research, at the National Energy Research Supercomputer Center (Berkeley, CA).

References and Notes

- (1) *Environmental Problems and Solutions: Greenhouse Effect, Acid Rain, Pollution*; Hemisphere: New York, 1990.
- (2) Adamson, A. W. *Physical Chemistry of Surfaces*, 5th ed.; Wiley-Interscience: New York, 1990.
- (3) Miranda, P. B.; Shen, Y. R. *J. Phys. Chem. B* **1999**, *103*, 3292.
- (4) Eiseenthal, K. B. *Chem. Rev.* **1996**, *96*, 1343.
- (5) Als-Nielsen, J.; Jacquemain, D.; Kjaer, K.; Leveiller, F.; Lahav, M.; Leiserowitz, L. *Phys. Rep.* **1994**, *246*, 252.
- (6) Bowers, J.; Zorbakhsh, A.; Webster, J. R. P.; Hutchings, L. R.; Richards, R. W. *Langmuir* **2001**, *17*, 140.
- (7) Benjamin, I. J. *Chem. Phys.* **1999**, *110*, 8070.
- (8) Tarek, M.; Tobias, D. J.; Klein, M. L. *Physica* **1996**, *A 231*, 117.

- (9) Morrone, J. A.; Tuckerman, M. E. *J. Chem. Phys.* **2002**, *117*, 4404.
- (10) Morrone, J. A.; Tuckerman, M. E. *Chem. Phys. Lett.* **2003**, *370*, 406.
- (11) Jorgenson, W. L. *J. Phys. Chem.* **1999**, *103*, 1276.
- (12) Caldwell, J. W.; Kollman, P. A. *J. Phys. Chem.* **1995**, *99*, 6208.
- (13) Gao, J.; Habibollahzadeh, D.; Shao, L. *J. Phys. Chem.* **1995**, *99*, 16460.
- (14) Yamaguchi, T.; Hidaka, K.; Soper, A. K. *Mol. Phys.* **1991**, *96*, 1159.
- (15) Tanaka, H.; Gubbins, K. E. *J. Chem. Phys.* **1992**, *97*, 2626.
- (16) Huang, J. Y.; Wu, M. H. *Phys. Rev. E* **1994**, *50*, 3737.
- (17) Matsumoto, M.; Takaoka, Y.; Kataoka, Y. *J. Chem. Phys.* **1993**, *98*, 1464.
- (18) Skaf, M. S.; Ladanyi, B. M. *J. Chem. Phys.* **1995**, *102*, 6542.
- (19) Laaksonen, A.; Kusalik, P. G.; Svishchev, I. M. *J. Phys. Chem. A* **1997**, *101*, 5910.
- (20) Soper, A. K.; Finney, J. L. *Phys. Rev. Lett.* **1993**, *71*, 4346.
- (21) Dixit, S.; Crain, J.; Poon, W. C. K.; Finney, J. L.; Soper, A. K. *Nature* **2002**, *416*, 829.
- (22) Dixit, S.; Soper, A. K.; Finney, J. L.; Crain, J. *Europhys. Lett.* **2002**, *59*, 377.
- (23) Guo, J.-H.; Luo, Y.; Augustsson, A.; Kashtanov, S.; Rubensson, J.-E.; Shuh, D. K.; Ågren, H.; Nordgren, J. *Phys. Rev. Lett.* **2003**, *91*, 157401.
- (24) Morita, A. *Chem. Phys. Lett.* **2003**, *375*, 1.
- (25) Souda, R.; Kawanowa, H.; Kondo, M.; Gotoh, Y. *J. Chem. Phys.* **2003**, *119*, 6194.
- (26) Wensink, E. J. W.; Hoffmann, A. C.; van Maaren, P. J.; van der Spoel, D. *J. Chem. Phys.* **2003**, *119*, 7308.
- (27) Ferrario, M.; Haughney, M.; McDonald, I. R.; Klein, M. L. *J. Chem. Phys.* **1990**, *93*, 5256.
- (28) Dang, L. X.; Chang, T.-M. *J. Chem. Phys.* **1997**, *106*, 8149.
- (29) Dang, L. X.; Chang, T.-M. *J. Chem. Phys.* **2003**, *119*, 9851.
- (30) Berendsen, H. J. C.; Postma, J. P. M.; van Gunsteren, W. F.; DiNola, A.; Haak, J. R. *J. Chem. Phys.* **1980**, *72*, 2384.
- (31) Ryckaert, J.-P.; Ciccotti, G.; Berendsen, H. J. C. *J. Comput. Phys.* **1977**, *23*, 327.
- (32) Matsumoto, M.; Kataoka, Y. *J. Chem. Phys.* **1988**, *88*, 3233.
- (33) Kirkwood, J. G.; Buff, F. P. *J. Chem. Phys.* **1949**, *17*, 338.
- (34) Wolfrum, K.; Graener, H.; Laubereau, A. *Chem. Phys. Lett.* **1993**, *213*, 41.
- (35) Chang, T.-M.; Dang, L. X. *J. Chem. Phys.* **1996**, *104*, 6772.
- (36) Du, Q.; Superfine, R.; Freysz, E.; Shen, Y. R. *Phys. Rev. Lett.* **1993**, *70*, 2313.
- (37) Dougan, L.; Bates, S. P.; Hargreaves, R.; Fox, J. P.; Crain, J.; Finney, J. L.; Reat, V.; Soper, A. K. *J. Chem. Phys.* **2004**, *121*, 6456.